Catalysis Today 170 (2011) 27–32

Contents lists available at ScienceDirect

Catalysis Today

journal homepage: www.elsevier.com/locate/cattod

Effect of trapped hydrogen on the induction period of cobalt–tungsten–boron/nickel foam catalyst in catalytic hydrolysis reaction of sodium borohydride

Hong-Bin Dai, Yan Liang, Ping Wang*

Shenyang National Laboratory for Materials Science, Institute of Metal Research, Chinese Academy of Sciences, 72 Wenhua Road, Shenyang 110016, PR China

ARTICLE INFO

Article history:
Available online 12 October 2010

Keywords:
Hydrogen storage
Sodium borohydride
Catalyst
Hydrolysis
Induction period

ABSTRACT

Calcination treatment is an important step in preparation of supported transition metal catalysts that are effective for promoting the hydrolysis reaction of sodium borohydride. We found that calcination treatment of cobalt–tungsten–boron/nickel foam catalysts results in the appearance of an induction period in their first time use, and the duration of which depends on the calcination temperature and atmosphere. Upon reusing the catalysts, the induction period completely disappeared. X-ray diffraction, scanning electron microscopy, X-ray photoelectron spectroscopy and synchronous thermal analyses techniques were employed to study the mechanism underlying the induction period phenomenon. Our study results showed that the appearance/disappearance of the induction period should be correlated with the desorption/reabsorption of hydrogen in the catalysts.

1. Introduction

Hydrogen storage is a major hurdle to the widespread implementation of the hydrogen fuel cell technologies [1]. Recently, on-demand hydrogen generation (HG) from chemical hydrides, in conjunction with spent fuel regeneration, has emerged as promising hydrogen storage means for transportation and portable applications. Sodium borohydride ($NaBH_4$) is a representative chemical hydride that has been extensively studied as a potential hydrogen storage medium [2–5]. $NaBH_4$ reacts with water following Eq. (1) (where x denotes the excess of water), yielding H_2 and borax

$$NaBH_4 + (2+x)H_2O \xrightarrow{\text{Catalyst}} NaBO_2 \cdot xH_2O + 4H_2 \uparrow + 210\,\text{kJ} \quad (1)$$

by-product. Since the hydrolysis reaction can be significantly accelerated by adding appropriate catalyst and effectively inhibited using alkaline stabilizer, the alkaline aqueous solution of $NaBH_4$ in combination with catalyst provides safe and compact hydrogen source with controllable HG performance [6]. But owing to the solubility limitation of borax by-product in aqueous solution and the "dead weight" H_2O existed in the hydration forms of $NaBO_2 \cdot xH_2O$, the $NaBH_4$-based hydrolysis system suffers low hydrogen density (typically 2–3 wt.%). This, together with the lack of energy- and cost-effective route for spent fuel regeneration, accounts for the "no-go" recommendation of US Department of Energy (DOE) for $NaBH_4$ for vehicular application. But fundamentally, the combined advantages of good fuel storability, reaction controllability, and the environmentally benign hydrolysis product make the $NaBH_4$-based hydrolysis system promising for portable or niche applications [4].

Catalyst study is a central issue in developing $NaBH_4$-based HG system. Besides acid accelerators, a number of noble or non-noble transition metals/alloys/salts have been identified to be catalytically active towards the hydrolysis reaction of $NaBH_4$, including Ru [6,7], Pt [8,9], Pt–Ru [10,11], Pt–Pd [12] or Pt–Pd–Ru [13], Ru–Co–Fe [14], Raney Ni and Co [15], Co and Ni borides [16–24], and so forth. These heterogeneous metal catalysts can greatly accelerate the hydrolysis reaction and yield nearly 100% conversion of $NaBH_4$ at ambient conditions. However, to meet the practical requirements for on-demand hydrogen generator, both the catalytic activity and durability of the catalysts need to be further improved. In this regard, a better understanding of the catalytic mechanism is clearly of significance for optimizing the composition, structure and preparation process of metal catalysts. Currently, the catalytic mechanism by which metal catalysts promote the hydrolysis reaction of $NaBH_4$ is still unclear, due primarily to the difficulties in obtaining direct and convincing evidences to depict the interaction between solid catalyst and liquid reactants [2,5,10,19,25–30]. Careful consideration of the related experimental phenomena is therefore important for gaining insight into the catalytic hydrolysis process.

In our recent study of catalytic hydrolysis of $NaBH_4$ using the cobalt–tungsten–boron catalyst supported on nickel foam (donated as Co–W–B/Ni foam catalyst hereinafter), we observed an interesting induction period phenomenon. It was found that the calcination treatment of the catalysts resulted in an induction period in their first time use. But upon reusing the catalysts, the induction period completely disappeared. A combination of property/structure studies has been carried out to understand this phenomenon.

* Corresponding author. Tel.: +86 24 2397 1622; fax: +86 24 2389 1320.
E-mail address: pingwang@imr.ac.cn (P. Wang).

0920-5861/$ – see front matter © 2010 Elsevier B.V. All rights reserved.
doi:10.1016/j.cattod.2010.09.007

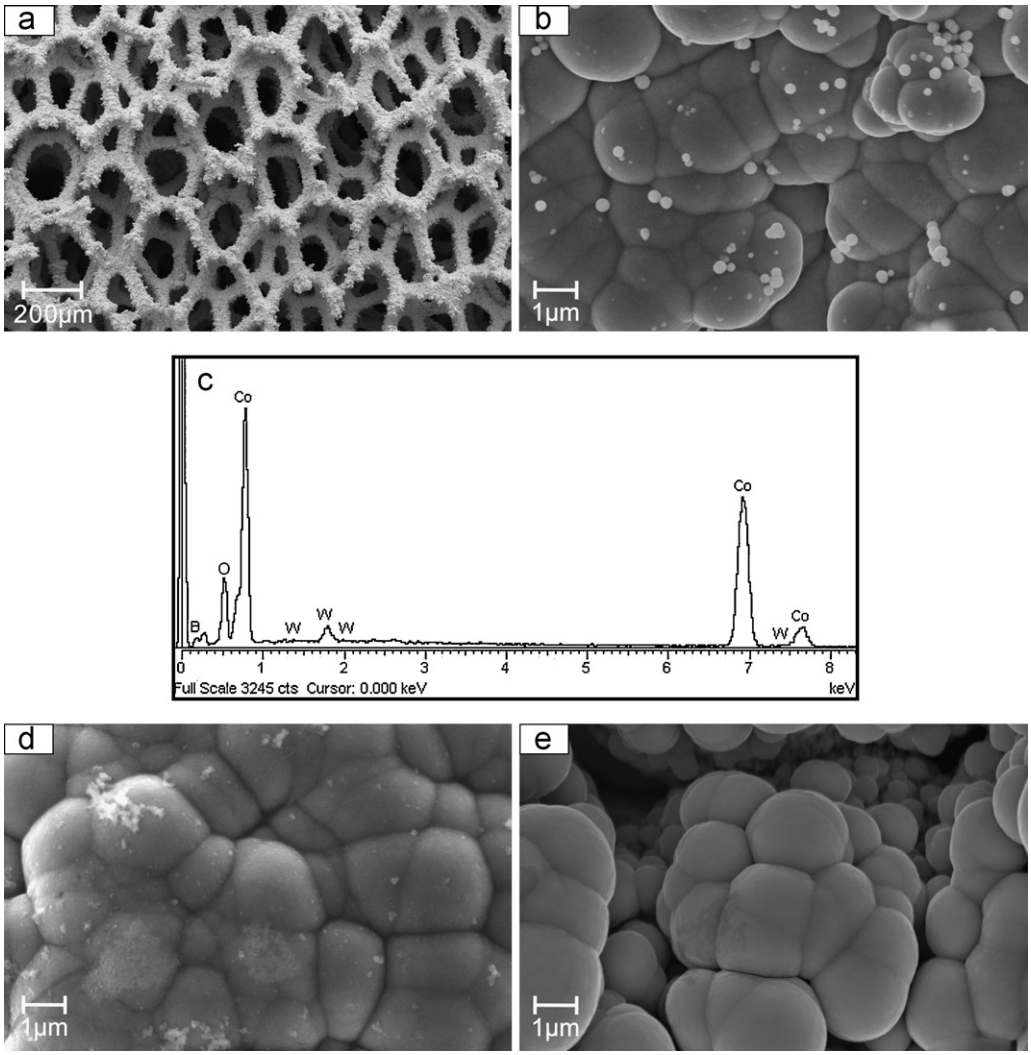

Fig. 1. SEM morphologies of the Co–W–B/Ni foam catalysts. (a) As-prepared catalyst at a low magnification; (b) as-prepared catalyst at a high magnification; (c) a representative EDX result of the catalyst; (d) post-calcined catalyst at 300 °C under Ar atmosphere; (e) the catalyst (d) after the first time use.

2. Experimental

2.1. Preparation and calcination of catalyst

The supported Co–W–B/Ni foam catalyst was prepared by using a modified electroless plating method, following a procedure detailed in Ref. [18]. The pretreated Ni foam was repeatedly plated in the bath solution for four times at 25 °C. The prepared black catalyst was washed thoroughly with deionized water and ethanol (99.9% purity) to remove the residual BH_4^-, Cl^-, NH_4^+ and Na^+ ions, and then dried in vacuum at 50 °C for 48 h, and stored in a vacuum desiccator. According to the weight change before and after plating, the Co–W–B catalyst loading is about 45 mg cm^{-2} (Ni foam).

The calcination treatment of the catalyst samples was carried out in a Sievert's type apparatus that was equipped with a programmed temperature controller, which allows a temperature controlling within ±1 °C. To minimize the H_2O/O_2 contamination during the calcination treatment, the reactor containing the catalyst sample was firstly evacuated/charged with Ar gas (99.999% purity) twice. The catalyst samples were then heated at a ramping rate of 2 °C min^{-1} to a designated temperature in the range of 100–400 °C, and held at that temperature for 2 h. In the case of calcination treatment under hydrogen atmosphere, the high-purity hydrogen gas (99.999% purity) was further purified using a hydrogen storage alloy system.

2.2. Catalytic hydrolysis performance testing

The HG amount and the HG rate of the hydrolysis system were measured using a classic water-displacement method. In a typical measurement, a fuel solution containing 20 wt.% $NaBH_4$ and 5 wt.% NaOH was thermostated in a sealed flask, and then one piece of Co–W–B/Ni foam catalyst (1 cm × 1 cm) attracted on a magnetic stirring bar was dropped into the solution to initiate hydrolysis reaction. The volume of the generated hydrogen was measured by monitoring the water displaced from a graduated cylinder (with a volume of 5.2 L) that was connected to the reaction flask.

2.3. Characterization of catalyst

The Co–W–B/Ni foam catalysts were characterized by powder X-ray diffraction (XRD, Rigaku D/max-2500, Cu Kα radiation) and scanning electron microscopy (SEM, LEO Supra 35) that is equipped with an energy dispersive X-ray (EDX) analysis unit (Oxford). The surface elements and their electronic states of the catalyst samples were analysed using X-ray photoelectron spectroscopy (XPS, ESCALAB 250, Al Kα X-ray source). All the binding energies were calibrated by using the C1s peak at 284.6 eV of the adventitious carbon as an internal standard. The curve fitting was performed by using XPS PEAK 4.1 software. The gas desorption behavior of the catalyst samples were analysed by synchronous thermal anal-

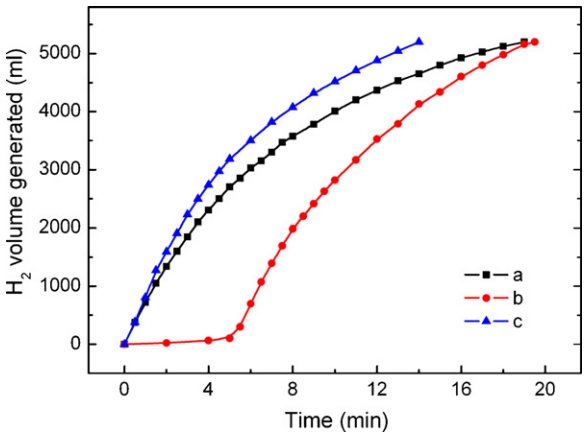

Fig. 2. HG kinetic curves of the fuel solution containing 20 wt.% $NaBH_4$ and 5 wt.% NaOH in the presence of Co–W–B/Ni foam catalyst (1 cm × 1 cm). (a) As-prepared catalyst; (b) post-calcined catalyst at 300 °C under Ar atmosphere; (c) post-calcined catalyst (b) in its second time use.

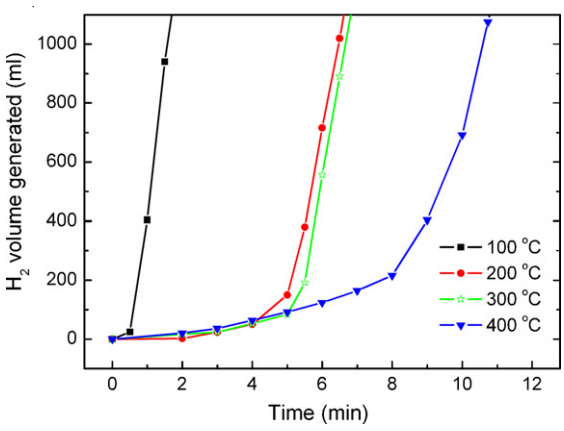

Fig. 3. Effect of calcination temperature on the induction duration of the Co–W–B/Ni foam catalysts in their first time use.

yses (thermogravimetry/mass spectrometer, TG/MS, Netzsch 449C Jupiter/QMS 403C). In the thermal analyses measurements, high-purity Ar (99.999% purity) was used as purge gas. The applied ramping rate was 10 °C min^{-1}.

3. Results and discussion

The supported Co–W–B/Ni foam catalyst can be readily prepared by using a modified electroless plating method [18]. Fig. 1(a) and (b) presents the SEM morphologies of the as-prepared catalyst. After repeating the plating process for four times, the Ni foam surface was completely covered by a catalyst coating layer composed of Co, W, B and O elements, as indicated by the EDX result shown in Fig. 1(c). Here, the O element in the catalyst coating layer should mainly come from oxidation of the catalyst upon exposure to air in the storage process [31]. The quantitative elemental analysis using inductively coupled plasma-atomic emission spectrometry (ICP-AES) determined that the catalyst coating contains 87 wt.% Co, 4.5 wt.% W and 8.5 wt.% B, corresponding to a formula of $Co_{65}W_1B_{34}$. As seen clearly in Fig. 1(b) at a high magnification, some small white particles with an average size of around 100 nm distribute randomly on the scraggy surface of the catalyst. Presumably, these small particles should be generated from the spontaneous decomposition of the plating solution in the catalyst preparation process. According to the ICP-AES analysis of the fine powder that was collected from the plating bath, these small particles possess similar chemical composition to the catalyst coating layer.

The supported transition metal catalysts are generally subjected to an appropriate calcination treatment to improve catalytic activity and the catalyst/support adhesion [16–18]. Here, our study found that the calcination treatment caused an interesting induction period phenomenon. As shown in Fig. 2, the as-prepared Co–W–B/Ni foam catalyst can initiate the hydrolysis reaction immediately upon contacting with the $NaBH_4$ solution. Examination of the kinetics curve found that the hydrolysis reaction reached its maximum rate from the initial stage. By contrast, the hydrolysis reaction system using the post-calcined catalyst showed a distinct induction period. But for the same catalyst in its second time use, the induction period was observed to completely disappear. Notably, this is a reproducible phenomenon, not only in the different batches of the Co–W–B/Ni foam catalysts, but also in other related transition metal catalysts, e.g. Co–B/Ni foam catalyst [17]. Additionally, comparison of the HG kinetics curves found that the calcined and reused catalysts were better than the as-prepared catalyst in terms of catalytic activity, which is presumably associated with the precipitation of nanocrystalline Co from the amorphous matrix [18], as elucidated in the XRD results shown below.

Further study found that the induction duration of the post-calcined catalysts in their first time use depends on the calcination conditions. Elevating the calcination temperature typically resulted in prolongation of the induction duration. As seen in Fig. 3, the induction duration of the Co–W–B/Ni foam catalyst increased from 0.5 to around 8 min upon increasing the calcination temperature from 100 to 400 °C under a vacuum condition. Changing the calcination atmosphere also produced considerable influence on the induction duration of the catalyst. As shown in Fig. 4, the post-calcined catalysts under Ar atmosphere or vacuum condition exhibit quite similar induction duration, both around 5 min. But upon using H_2 atmosphere in the calcination treatment, the induction duration of the calcined catalyst became shorter. Particularly, when the calcination was carried out under 5.0 MPa hydrogen, the induction duration was reduced to around 2 min, just about 1/3 of that of the calcined catalyst under Ar atmosphere. In all cases, the induction period of the calcined catalysts disappeared in their second time use, regardless of the calcination conditions applied.

As a start of the mechanism study, we examined the catalyst samples at different states by using XRD and SEM. Unfortunately, these phase/structure analyses provide no valuable hint for understanding the induction period phenomenon. Fig. 5 presents the

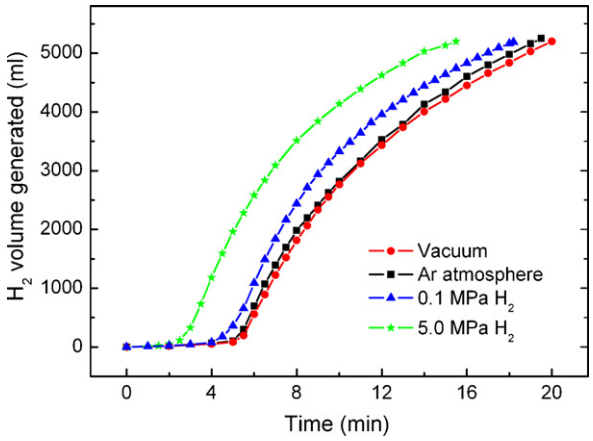

Fig. 4. Effect of calcination atmosphere or pressure on the induction duration of the Co–W–B/Ni foam catalysts in their first time use. The calcination temperature was 300 °C.

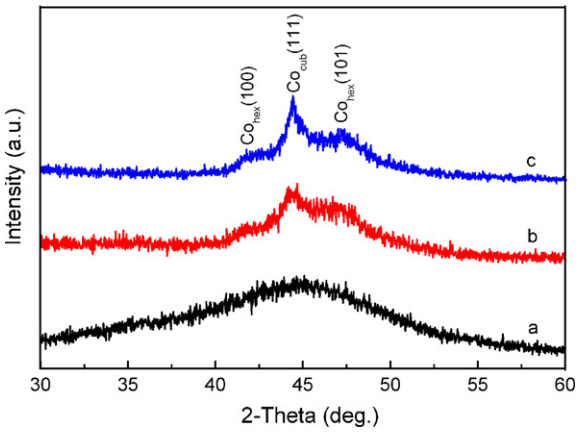

Fig. 5. XRD patterns of the Co–W–B/Ni foam catalysts. (a) As-prepared catalyst; (b) post-calcined catalyst at 300 °C under Ar atmosphere; (c) the catalyst (b) after its first time use.

XRD patterns of the Co–W–B/Ni foam catalysts at different states. The wide and diffuse peak centered at around $2\theta = 45°$ clearly indicated the amorphous nature of the as-prepared Co–W–B catalyst. After being calcined at 300 °C for 2 h, the catalyst showed weak diffraction peaks at around $2\theta = 44.4°$, indicative of the formation of nanocrystalline Co. As the post-used catalyst exhibited similar diffraction pattern to the post-calcined catalyst, the formation of nanocrystalline Co should have no relevance to the induction period. Additionally, the catalyst samples at as-prepared, post-calcined and reused states, respectively, showed similar morphological feature, as shown in Fig. 1(b), (d) and (e). This study results clearly suggested that the appearance/disappearance of induction period should originate from some subtle structure and/or composition changes that occurred in the calcination or hydrolysis reaction processes.

The first possibility that comes to our mind is that the induction period phenomenon is correlated with the changed surface oxidation state of the catalyst. The calcination treatment may aggravate surface oxidation of the catalyst via promoting the reactions between the physisorbed H_2O/O_2 and the component elements of the catalyst. The formed oxidation layer may block the contact between fuel solution and catalyst, thus prohibiting the occurrence of hydrolysis reaction . But upon contacting with the reductive $NaBH_4$ solution, the metal oxides layer might be reduced back to elemental metal or alloy [20,22,30] and accordingly, the catalytic activity of the catalyst is recovered. To check this possibility, we examined and compared surface element chemical state of different catalyst samples. Fig. 6 presents the XPS spectra of the catalyst samples, from which the binding energies of the surface elements were determined and summarized in Table 1. The as-prepared catalyst exhibits considerable surface oxidation, as evidenced by the clear identification of CoO (781.5/797.1 eV), WO_3 (35.1/37.2 eV) and B_2O_3 (191.9 eV) species [22,31,32]. But meanwhile, metallic Co (778.5/793.5 eV) and B (188.0 eV) remained detectable. Air exposure caused further aggravated surface oxidation. For the catalyst sample after air exposure for one week, only oxidized species were observed on the surface, which possess amorphous nature according to the XRD analysis. In the post-calcined catalyst sample under Ar atmosphere, we identified W 4f and B 1s peaks that resemble those in the air-exposed sample. But according to the Co 2p spectrum, there existed metallic Co^0 on the surface of the calcined catalyst, which agrees well with the XRD results, as seen in Fig. 6(b). In the post-calcined catalyst sample under 5.0 MPa H_2, the metallic state signals of all the component elements were detectable. As a whole, XPS studies showed that air exposure for one week causes more

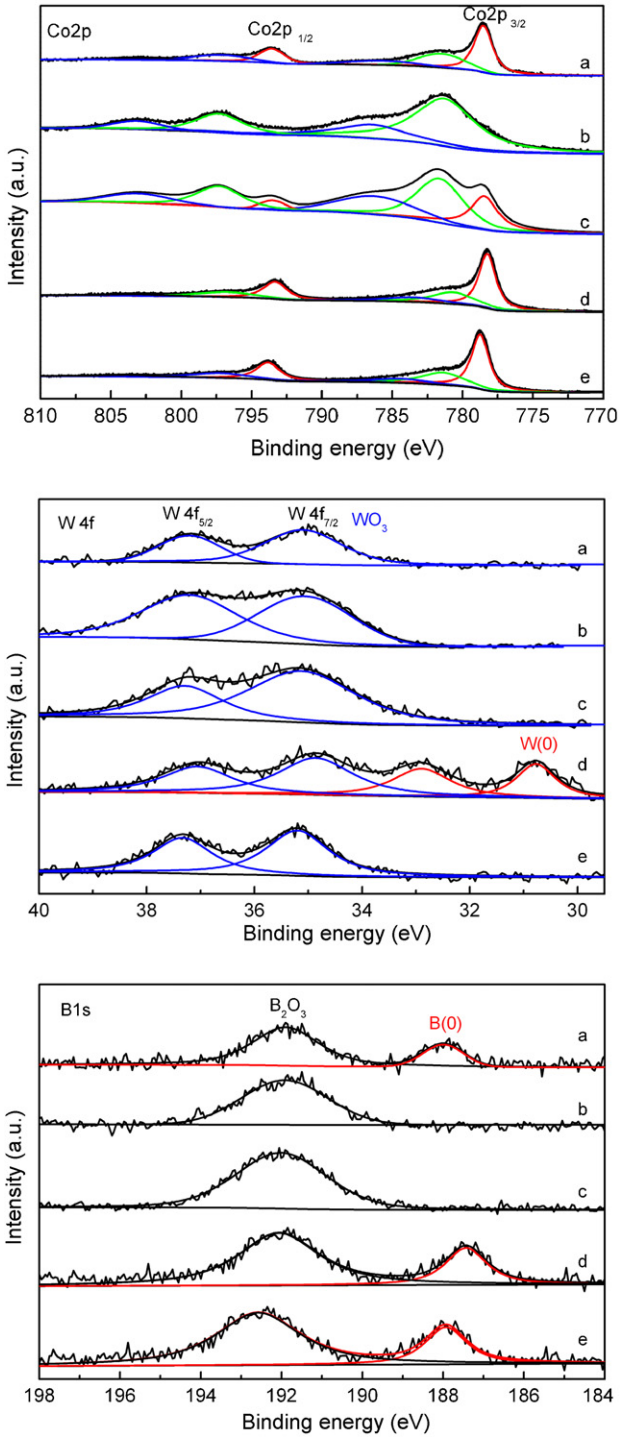

Fig. 6. XPS spectra of the Co–W–B/Ni foam catalysts. (a) As-prepared; (b) as-prepared catalyst followed by air exposure for one week; (c) post-calcined catalyst at 300 °C under Ar atmosphere; (d) post-calcined catalyst at 300 °C under 5.0 MPa H_2; (e) the catalyst (b) after immersing in the $NaBH_4$ solution for 30 s.

serious surface oxidation of the Co–W–B catalyst than calcination treatment at 300 °C for 2 h. Among the five examined samples (a–e), the post-calcined catalyst under 5.0 MPa H_2 exhibited the lightest surface oxidation. But according to the property examinations, the air-exposed catalysts showed no induction period (Fig. 7), whereas the calcined catalysts, even under H_2 atmosphere, exhibited an induction period in their first time use (Fig. 4). These findings clearly indicate that surface oxidation is not the main reason for the appearance of induction period. Actually, designed experiments

Table 1
XPS binding energies (eV) for the Co–W–B/Ni foam catalysts.

Catalyst sample	Co $2p_{3/2}$		Co $2p_{1/2}$		W $4f_{7/2}$	W $4f_{5/2}$	B 1s
	MP	SP	MP	SP			
a	778.5		793.5		35.1	37.2	188.0
	781.5	786.0	797.1	803.1			191.9
b	781.4	786.3	797.2	803.1	35.1	37.2	191.9
c	778.4		793.4		35.2	37.3	192.0
	781.6	786.2	797.2	803.0			
d	778.2		793.3		30.8	32.9	187.4
	780.7	785.5	796.7	803.3	34.9	37.1	192.1
e	778.7		793.8		35.2	37.3	187.9
	781.4	784.6	797.2	803.6			192.1

(a) As-prepared catalyst; (b) as-prepared catalyst followed by air exposure for one week; (c) post-calcined catalyst at 300 °C under Ar atmosphere; (d) post-calcined catalyst at 300 °C under 5.0 MPa H_2; (e) the catalyst (b) after immersing in the $NaBH_4$ solution for 30 s. MP = binding energy of main peak, SP = binding energy of satellite peak.

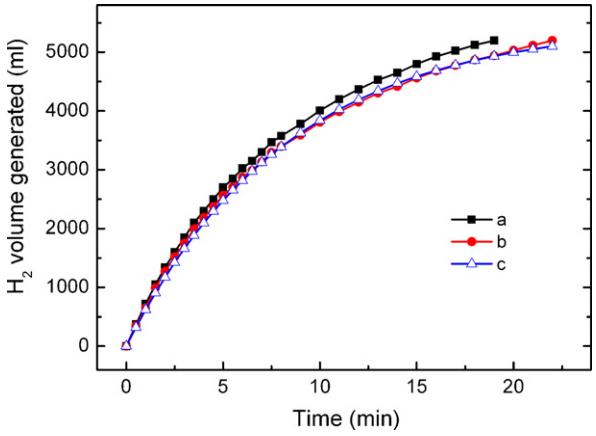

Fig. 7. Comparison of HG kinetics of the fuel solution containing 20 wt.% $NaBH_4$ and 5 wt.% NaOH in the presence of Co–W–B/Ni foam catalyst (1 cm × 1 cm). (a) As-prepared; (b) as-prepared catalyst followed by air exposure for one week; (c) as-prepared catalyst followed by air exposure at 50 °C for 50 h.

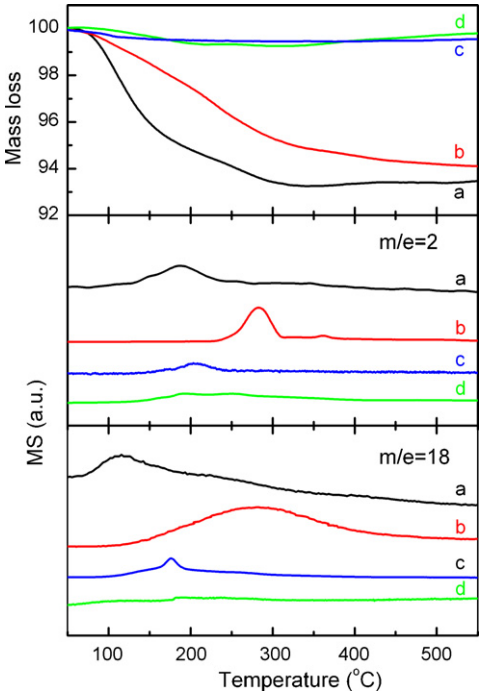

Fig. 8. TG/MS results of the Co–W–B catalyst samples at different states. (a) As-prepared; (b) post-calcined catalyst after its first time use; (c) post-calcined catalyst at 300 °C under 5.0 MPa H_2; (d) post-calcined catalyst at 300 °C under Ar atmosphere.

showed that surface oxidation exerts quite limited influence on the catalytic activity of the Co–W–B catalysts. As seen in Fig. 7, the catalyst samples after air exposure for one week or after being heated at 50 °C under air for 50 h exhibited quite similar catalytic performance to the as-prepared catalyst. The reason for this phenomenon is that the Co oxides can be readily reduced back to the corresponding metallic states upon contacting with the reductive $NaBH_4$ solution [22], as seen in Fig. 6(e).

Alternatively, comprehensive understanding of the experimental results led us to a speculation that the observed induction period phenomenon may correlate with the trapped hydrogen in the catalyst samples. Similar hypothesis was also proposed by Burchardt et al. in their study of alkaline water hydrolysis using NiP_x catalyst [33,34]. Their study clearly showed that the catalytic activity correlated closely with the hydrogen content in the NiP_x alloys. In the present study, hydrogen trapping in the Co–W–B catalyst was directly evidenced by the synchronous TG/MS results, as presented in Fig. 8. In the as-prepared catalyst, a H_2-desorption peak was observed to start from ~100 °C, and reached its maximum at around 180 °C. As the peak temperature of H_2-release was substantially higher than that of the H_2O-desoprtion peak (at around 110 °C), the H_2-signal can be safely ascribed to hydrogen release from the catalyst sample. After being calcined at 300 °C, the catalyst samples exhibited significantly weakened MS H_2-signals. A close examination found that H_2-signal from the post-calcined catalyst under 5.0 MPa H_2 was stronger than that from the calcined catalyst under Ar atmosphere. Interestingly, the hydrogen-trapping in the Co–W–B catalyst is a "reversible" phenomenon. As seen in the MS H_2-pattern (b), the post-calcined catalyst showed again a strong H_2-signal after its first time use. Correlating these MS results with the property examination results suggests that hydrogen desorption/reabsorption is a mechanistic reason for the appearance/disappearance of the induction period in the catalyst samples. In this regard, the observed effect of H_2 atmosphere on shortening the induction duration might be understood from the restrained hydrogen release from the catalyst sample under H_2 atmosphere. Unfortunately, owing to the concurrent release of H_2O, it is impossible to quantitatively correlate the induction duration with the residual hydrogen content in the catalyst. Additionally, it was noticed that the hydrogen desorption behavior of the reused catalyst differed from that of the as-prepared catalyst. This finding suggests that hydrogen-trapping in the transition metal catalyst is a complicated phenomenon, which may involve different trapping sites and/or interaction modes. In this regard, detailed experimental/theoretical studies are still required to further mechanistic understanding.

Correlating the induction period phenomenon with the hydrogen-trapping in the catalyst samples provides valuable insight into the catalytic hydrolysis mechanism. Currently, it is generally accepted that metal (M) – catalysed hydrolysis of $NaBH_4$

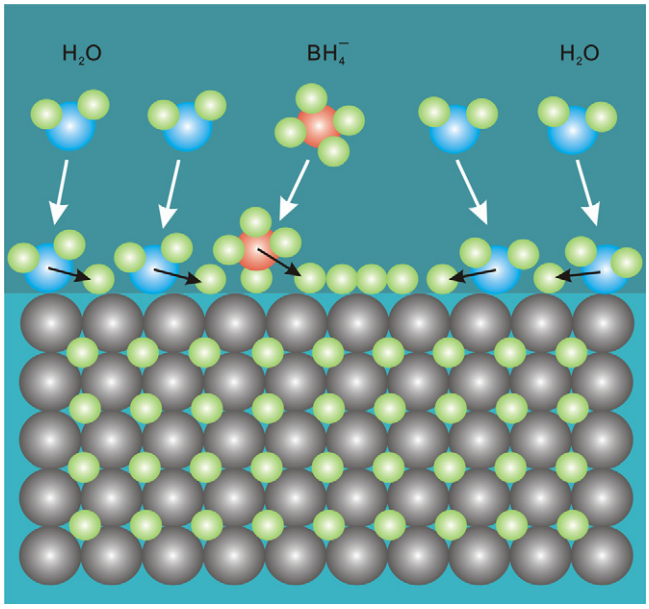

Fig. 9. Schematic diagram of hydrogen absorption/trapping in the metallic catalyst.

involves the dissociative chemisorption of BH_4^- on the catalyst surface as the first kinetic step [10,12,19,25–29]. The resulting MBH_4^- complex then dissociates to form $M–BH_3^-$ and M–H intermediates. According to Holbrook and Twist [25], $M–BH_3^-$ subsequently reacts with H_2O, possibly via a BH_3 intermediate, to generate $BH_3(OH)^-$ and M–H species. The former undergoes stepwise replacement of B–H bonds by $B–OH^-$ bonds, and finally yields $B(OH)_4^-$; the latter combines with another M–H to afford H_2 and to regenerate the active sites. Alternatively, Peña-Alonso et al. [12] suggested that transfer of the negative charge of $M–BH_3^-$ to H of M–H is a critical mechanistic step. The negatively charged H reacts with H_2O to form H_2 and OH^-. The generated OH^- then participates in the stepwise replacement of the hydridic H bonded in B, resulting in the formation of $B(OH)_4^-$ product. Whereas differing in the understanding of mechanistic pathway, both models emphasized the catalysis reactions on the metal catalyst surface. Here, our studies show that the catalytic hydrolysis process involves not only the surface reactions, but also the trapping and bulk diffusion of hydrogen in the metal catalysts. In preparation of the catalyst using electroless plating method, the deposition of catalyst coating is accompanied with vigorous hydrogen evolution [17,18]. The metal catalysts in their as-prepared states absorb a certain amount of hydrogen, which may exist in atomic state and occupy the interstitial sites of metal lattice or grain boundary. These trapped hydrogen atoms may play a crucial role in catalytic hydrolysis reaction of $NaBH_4$ through providing a H-saturated environment of the catalysts. In the case of pre-desorption of the trapped hydrogen in the calcination treatment processes, the detached H from BH_4^- or H_2O may be firstly absorbed on the catalyst surface and then migrate into the bulk of the catalyst, as schemed in Fig. 9. Here, designed experiments using deuterated species may provide valuable insight into the origin of the trapped hydrogen in the catalyst. The observed induction period might be understood as the time required for reaching the saturated H-concentration in the catalysts. When the saturated H-concentration is reached in the bulk of the catalyst, HG should occur mainly on the catalyst surface via combination of H atoms. Currently, the mechanism underlying the hydrogen absorption in metal catalysts and the correlation between the resulted changes of electronic structure and catalytic activity remain unclear. Further detailed studies are still required.

4. Conclusions

Our studies found that calcination of the Co–W–B/Ni foam catalyst results in the appearance of induction period in its first time use, and the duration of which depends on the calcination temperature and atmosphere. The induction duration of the catalyst can be shortened by using high-pressure H_2 in the calcination process, and eliminated upon reusing the catalyst. A combination of structural and property studies suggest that the appearance/disappearance of the induction period should be correlated with the trapped hydrogen in the catalyst, rather than the changes of surface oxidation state of the catalyst. This experimental finding provides insight into the catalytic hydrolysis mechanism of $NaBH_4$.

Acknowledgements

The financial supports for this research from the National High-Tech. R&D Program of China (863 Program, Grant No. 2009AA05Z109), the National Basic Research Program of China (973 program, Grant No. 2010CB631305), the National Natural Science Foundation of China (Grant No. 51071155) and the Frontier Project of CAS Knowledge Innovation Program (Grant No. KGCXZ-YW-342) are gratefully acknowledged.

References

[1] L. Schlapbach, A. Züttel, Nature 414 (2001) 353.
[2] P. Wang, X.D. Kang, Dalton Trans. 40 (2008) 5400.
[3] U.B. Demirci, O. Akdim, J. Andrieux, J. Hannauer, R. Chamoun, P. Miele, Fuel Cells 10 (2010) 335.
[4] U.B. Demirci, O. Akdim, P. Miele, Int. J. Hydrogen Energy 34 (2009) 2638.
[5] B.H. Liu, Z.P. Li, J. Power Sources 187 (2009) 527.
[6] S.C. Amendola, S.L. Sharp-Goldman, M.S. Janjua, N.C. Spencer, M.T. Kelly, P.J. Petillo, M. Binder, Int. J. Hydrogen Energy 25 (2000) 969.
[7] C.L. Hsueh, C.Y. Chen, J.R. Ku, S.F. Tsai, Y.Y. Hsh, F.H. Tsau, M.S. Jeng, J. Power Sources 177 (2008) 485.
[8] Y. Kojima, K. Suzuki, K. Fukumoto, M. Sasaki, T. Yamamoto, Y. Kawai, H. Hayashi, Int. J. Hydrogen Energy 27 (2002) 1029.
[9] U.B. Demirci, F. Garin, Int. J. Green Energy 5 (2008) 148.
[10] U.B. Demirci, F. Garin, J. Alloys Compd. 463 (2007) 107.
[11] P. Krishnan, T.H. Yang, W.Y. Lee, C.S. Kim, J. Power Sources 143 (2005) 17.
[12] R. Peña-Alonso, A. Sicurelli, E. Callone, G. Carturan, R. Raj, J. Power Sources 165 (2007) 315.
[13] L. Hu, R. Ceccato, R. Raj, J. Power Sources 196 (2011) 741.
[14] J.H. Park, P. Shakkthivel, H.J. Kim, M.K. Han, J.H. Jang, Y.R. Kim, H.S. Kim, Y.G. Shu, Int. J. Hydrogen Energy 33 (2008) 1845.
[15] B.H. Liu, Z.P. Li, S. Suda, J. Alloys Compd. 415 (2006) 288.
[16] J. Lee, K.Y. Kong, C.R. Jung, E. Cho, S.P. Yoon, J. Han, T.G. Lee, S.W. Nam, Catal. Today 120 (2007) 305.
[17] H.B. Dai, Y. Liang, P. Wang, H.M. Cheng, J. Power Sources 177 (2008) 17.
[18] H.B. Dai, Y. Liang, P. Wang, X.D. Yang, T. Rufford, M. Lu, H.M. Cheng, Int. J. Hydrogen Energy 33 (2008) 4405.
[19] H.B. Dai, Y. Liang, L.P. Ma, P. Wang, J. Phys. Chem. C 112 (2008) 15886.
[20] J. Andrieux, D. Swierczynski, L. Laversenne, A. Garron, S. Bennici, C. Goutaudier, P. Miele, A. Auroux, B. Bonnetot, Int. J. Hydrogen Energy 34 (2009) 938.
[21] A. Garron, S. Bennici, A. Auroux, Appl. Catal. A: Gen. 378 (2010) 90.
[22] N. Patel, R. Fernandes, A. Miotello, J. Catal. 271 (2010) 315–324.
[23] R. Chamoun, U.B. Demirci, D. Cornu, Y. Zaatar, A. Khoury, R. Khoury, P. Miele, Appl. Surf. Sci. 256 (2010) 7684.
[24] N. Patel, R. Fernandes, N. Bazzanella, A. Miotello, Thin Solid Films 518 (2010) 4779.
[25] K.A. Holbrook, P.J. Twist, J. Chem. Soc. A 15 (1971) 890.
[26] C.M. Kaufman, B. Sen, J. Chem. Soc., Dalton Trans. (1985) 307.
[27] Y.V. Larichev, O.V. Netskina, O.V. Komova, V.I. Simagina, Int. J. Hydrogen Energy 35 (2010) 6501.
[28] G. Guella, C. Zanchetta, B. Patton, A. Miotello, J. Phys. Chem. B 110 (2006) 17024.
[29] G. Guella, B. Patton, A. Miotello, J. Phys. Chem. C 111 (2007) 18744.
[30] P. Krishnan, K.L. Hsueh, S.D. Kim, Appl. Catal. B: Environ. 77 (2007) 206.
[31] W.L. Dai, M.H. Qiao, J.F. Deng, Appl. Surf. Sci. 120 (1997) 119.
[32] B.J. Tan, K.J. Klabunde, P.M.A. Sherwood, J. Am. Chem. Soc. 113 (1991) 855.
[33] T. Burchardt, V. Hansen, T. Våland, Electrochim. Acta 46 (2001) 2761.
[34] T. Burchardt, Int. J. Hydrogen Energy 26 (2001) 1193.